Interpretation of Kelvin/Rossby waves in the equatorial Pacific from model-Geosat data intercomparison during the 1986-1987 El Niño

Equatorial waves
Model
Satellite altimetry
El Niño
Geosat

Ondes équatoriales
Modèle
Altimétrie satellitaire
El Niño
Geosat

Yves du PENHOAT, Thierry DELCROIX and Joël PICAUT

Groupe SURTROPAC, Institut Français de Recherche Scientifique pour le Développement en Coopération (ORSTOM), B. P. A5, Nouméa, New Caledonia.

ABSTRACT

Analysis of Geosat sea level data over the period November 1986-November 1987 has evidenced long, low-frequency equatorial wave propagations over most of the equatorial Pacific basin (Delcroix *et al.*,1991). The succession of downwelling Kelvin, upwelling Kelvin, and upwelling Rossby waves has raised a series of questions. Is the observed upwelling Rossby wave due to a reflection process on the eastern boundary, or due to wind forcing near the equator? Why is there no evidence of a reflection of the downwelling Kelvin wave? Is this wave sequence a feature of the 1986-1987 El Niño phenomenon or is it to be found in the mean seasonal cycle?

We used a linear model forced by the FSU wind stress to study these questions. The results, during the period November 1986-November 1987, show the successive downwelling/ upwelling Kelvin waves and upwelling Rossby wave as in the Geosat observations. Another test was made, using only the part of the forcing responsible for creating Kelvin waves, in order to evaluate the portion of the signals that was due to the reflection process and the part due to local forcing. It appears that wind forcing favourable to upwelling in the eastern part of the equatorial basin is the main mechanism which both generates the upwelling Rossby wave and inhibits the reflection of the downwelling Kelvin wave. However, the reflection of the upwelling Kelvin wave contributes to the upwelling Rossby wave signal, and makes it visible all the way from the eastern to the western sides of the equatorial Pacific. Results of a climatological run show that the successive downwelling/upwelling Kelvin and Rossby wave propagations are present in the mean seasonal cycle. However, the corresponding model signals, as well as the wind forcing anomalies, show a larger amplitude in 1986-1987.

Oceanologica Acta, 1992. **15**, 5, 545-554.

RÉSUMÉ

Interprétation, à l'aide d'un modèle, des ondes équatoriales de Kelvin et Rossby détectées par Geosat au cours de l'El Niño 1986-1987

L'analyse du niveau de la mer déduit des mesures du satellite Geosat, pendant la période novembre 1986-novembre 1987, a montré la présence d'ondes longues équatoriales de basse fréquence se propageant dans la majeure partie de l'Océan Pacifique équatorial (Delcroix *et al.*, 1991). La succession d'ondes de Kelvin de downwelling et d'upwelling et d'une onde de Rossby d'upwelling soulève une série de questions. L'onde de Rossby d'upwelling est-elle générée par une réflexion sur le bord est de l'océan ou directement par le forçage du vent au voisi-

nage de l'équateur ? Pourquoi n'observe-t-on pas la réflexion de l'onde de Kelvin de downwelling ? La séquence d'ondes observée est-elle caractéristique de l'événement El Niño 1986-1987, ou bien peut-elle être détectée dans le cycle saisonnier moyen ?

Un modèle linéaire est utilisé pour répondre à ces questions. Les résultats du modèle, forcé par les vents FSU mesurés pendant la période novembre 1986-1987, montrent la succession des ondes de Kelvin de downwelling et d'upwelling et de l'onde de Rossby d'upwelling, semblable aux observations déduites de Geosat. Un autre test est effectué en utilisant uniquement la partie du forçage responsable de la genèse des ondes de Kelvin, afin d'évaluer la part des signaux due aux processus de réflexion et due au forçage local. Il s'avère que le forçage du vent, favorable à l'upwelling dans la partie est du bassin, est le principal mécanisme qui, à la fois, génère l'onde de Rossby d'upwelling et inhibe la réflexion de l'onde de Kelvin de downwelling. Enfin, en forçant le modèle avec des vents climatologiques, on montre que la succession d'ondes de Kelvin et de Rossby de downwelling/upwelling existe également dans le cycle saisonnier moyen. Cependant, les signaux correspondants ont une amplitude plus importante en 1986-1987, de même que les anomalies du forçage.

Oceanologica Acta, 1992. **15**, 5, 545-554.

INTRODUCTION

The importance of low-frequency equatorial waves in the adjustment of the ocean to wind forcing has been widely documented since the seminal work of Cane and Sarachick (1977; 1981). Equatorial waves have received particular attention in theoretical studies based on the idea that the El Niño sea level (or heat content) signal is largely a linear dynamic response to wind forcing. Equatorial Kelvin and long Rossby waves are the only important wave types relevant to El Niño time and space scales. They play a key role in numerical models forced by surface wind stress and they account for the evolution of El Niño (*e. g.*, Busalacchi and O'Brien, 1981; Busalacchi and Cane, 1985). However, their detection is not straightforward. If the forcing has a scale large enough compared to the ocean size and/or a slow temporal evolution, the ocean response would result in a combination of forced and free motions. Wave propagations would then be hardly detectable. In contrast, during periods when trade winds collapse or when energetic westerlies appear in the western equatorial Pacific, wave propagations might be traced across the ocean basin.

The success of equatorial theory has encouraged the search for signature of equatorial Kelvin and Rossby waves in oceanic data. For instance, equatorial Kelvin waves have been detected in the tropical Pacific Ocean through their signature in current records (Knox and Halpern, 1982) or sea level changes (Lukas *et al.*, 1984). Annual long baroclinic Rossby waves have also been discovered in the northern tropical Pacific using pycnocline or isotherm depth variations deduced from BT and XBT (eXpendable Bathy Thermograph) measurements (Meyers, 1979; Kessler, 1990).

Due to the scarcity of oceanic observations regarding the basin size, it is difficult to trace equatorial waves all across the Pacific Ocean. Observations are made at single mooring locations, or during oceanographic cruises and along XBT transects, and they usually are not synoptic. This difficulty has been overcome recently with the opening of the era of instrument-bearing satellites. Satellite altimeter measurements do, in fact, provide the only means of obtaining long sea level time series over a whole oceanic basin. For example, the US Navy Geosat altimeter data, available over the period 1985-1989 (Douglas and Cheney, 1990), have provided the first opportunity for comprehensive sea level monitoring.

Understanding of the 1986-1987 El Niño, observed and described by means of classical oceanographic instruments (*e. g.*, McPhaden and Hayes, 1990; Delcroix *et al.*, 1992), has greatly benefited from studies drawing on the Geosat time/space coverage. For example, Miller *et al.* (1988) and Delcroix *et al.* (1991) have detected propagation of a downwelling Kelvin wave along the equator. The Kelvin wave is forced by westerly wind anomalies in the western Pacific in November 1986. It results in positive (10-15 cm) sea level anomalies relative to the November 1986-November 1987 time period. Delcroix *et al.* (1991) (hereafter referred to as DPE) have also detected propagation of an upwelling equatorial Kelvin wave (leading to negative sea level anomalies) in February-March 1987. They further describe the westward propagation of a first meridional mode Rossby wave, clearly evident in sea level variations along the 4°N and 4°S parallels. They deduce, by four independent estimates, that the phase speed and meridional scale of these waves have the characteristics of a first baroclinic mode with mean phase speed c = 2.68 m/s. Interestingly, zonal geostrophic surface current anomalies, estimated from Geosat sea level data, compare realistically with low-frequency current variations observed at the equator (Picaut *et al.*, 1990). Current anomalies associated with propagations of the Kelvin and Rossby waves have been calculated, reaching as much as 80 cm/s. Therefore, wave propagations are likely to play a role in the 1986-1987 El Niño evolution, through air-sea interaction changes induced by displacement of sea surface temperature patterns.

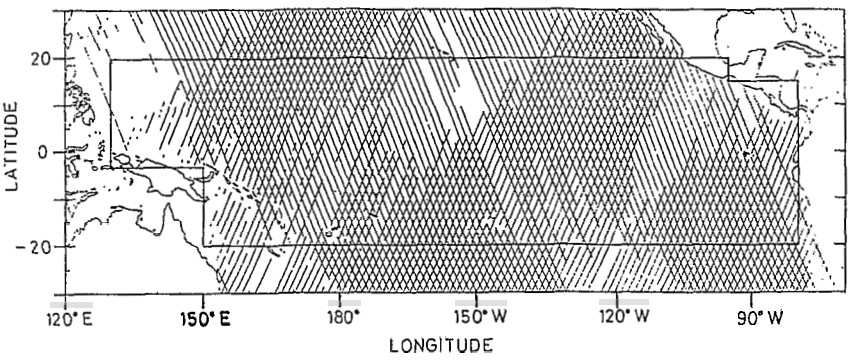

Figure 1

Ground tracks of the Geosat 17-day repeat orbit over the tropical Pacific Ocean. The heavy line denotes the model boundary.

Traces au sol de l'orbite répétitive de Geosat (17 jours) sur l'Océan Pacifique tropical. Les frontières du modèle sont matérialisées en traits gras.

In their conclusion, DPE suggest a tentative explanation for the generation of the waves. In particular, they raise three questions they cannot solve with the limited Geosat data set. Firstly, due to the correspondance in timing, does the equatorial upwelling Rossby wave issue from the reflection of the upwelling Kelvin wave? Secondly, why is there no sea level signature of the reflection of the downwelling Kelvin wave on the eastern boundary in January 1987? Thirdly, does this wave activity characterize the 1986-1987 El Niño or is it part of the "normal" mean seasonal cycle ?

In this paper, a numerical model is utilized to answer the above questions. It is a simple linear model that has been extensively used and which has proved to be adequate in interpreting sea level variations, and dynamic height at seasonal and interannual time scales (*e. g.*, du Penhoat and Tréguier, 1985; Busalacchi and Cane, 1985). Its efficient numerical scheme makes it possible to identify processes thought to be important in interpreting the ocean response to wind forcing.

This paper is organized as follows: the model is described in the next section following a brief review of DPE's Geosat data analysis. Comparison and analysis of the modelled and Geosat-derived sea level anomalies are presented in the third section. The model results are then interpreted with special attention to wave reflection processes. Finally, the 1986-1987 El Niño wave signal is compared to the mean seasonal cycle.

OBSERVATIONS AND MODEL

As in DPE, the Geosat data referred to in the present study correspond to the first 22 repeated cycles of the Exact Repeat Mission (ERM; 8 November 1986 to 18 November 1987). These data were originally provided by Dr. Koblinsky (NASA/Goddard Space Flight Center), and further processed in ORSTOM-Nouméa, to retain gridded low-frequency sea level anomalies relative to the ERM period. Detailed information about the Geosat data, and their processing and gridding, can be found in DPE. These authors have made comparisons between Geosat sea level anomalies and various estimates of surface dynamic height anomalies. In agreement with Cheney *et al.* (1989), they found rms differences varying from 3 to 3.8 cm. Analysed signals in DPE are then strong enough to demonstrate that the major large-scale, low-frequency sea level changes (as well as zonal surface geostrophic current) can be explained in light of the linear equatorial wave theory.

The model is a linear wind-forced model and details of the solution procedure can be found in Cane and Patton (1984). Briefly, the linear shallow water equations are solved on an equatorial β-plane, subject to the low-frequency, long-wave approximation. The Kelvin wave contribution to the solution is determined by integration along the characteristics. The contribution of long Rossby waves is calculated using an implicit finite difference scheme. Variables are located on a staggered grid of 2° longitude by 0.5° latitude, and a five-day time step is used to fit the Geosat time grid defined in DPE. The model basin is bounded at 130°E and 80°W, 20°N and 20°S.The coast of Central America is approximated by a 5° latitude x 15° longitude rectangle on the northeast corner of the basin, and the coasts of Papua-New Guinea and Australia by a 17° latitude x 20° longitude rectangle in the southwest corner of the basin (Fig. 1). Based on DPE's estimates, the model is run with a characteristic internal wave speed c = 2.68 m/s, *i. e.*, an equivalent depth of 74 cm.

The forcing is derived from the Florida State University (FSU) pseudo-stress product (Goldenberg and O'Brien, 1981). Monthly pseudo-stress components, available on a 2°x 2° grid, are linearly interpolated to the model time and space grids. A drag coefficient of 1.3×10^{-3} is used to convert pseudo-stress to wind stress values. The model is run from 1961 to 1987, which provides a sufficient spin up time for low latitude transients to die out. Model pycnocline depth anomalies are then computed relative to the November 1986-November 1987 period for consistency with Geosat sea level anomalies.

With one vertical mode, the model is formally similar to a reduced-gravity two-layer system with an active layer of density ρ over a deep layer at rest of density ρ + Δρ (Cane, 1984). Hence, to compare with the Geosat-derived sea level, modelled pycnocline depth variations Δh are converted to sea level variations Δη using the relation:

$$\Delta\eta = - \Delta h \, \rho^{-1} \, \Delta\rho$$

with $\Delta\rho/\rho = 5 \, 10^{-3}$, a mean observed value (Rébert *et al.*, 1985).

COMPARISON

Previous studies with similar linear models (*e. g.*, Busalacchi and Cane, 1985) have shown good concordance between modelled and observed *in situ* sea level variations. This was confirmed in the present study through various types of comparisons. These comparisons are not shown

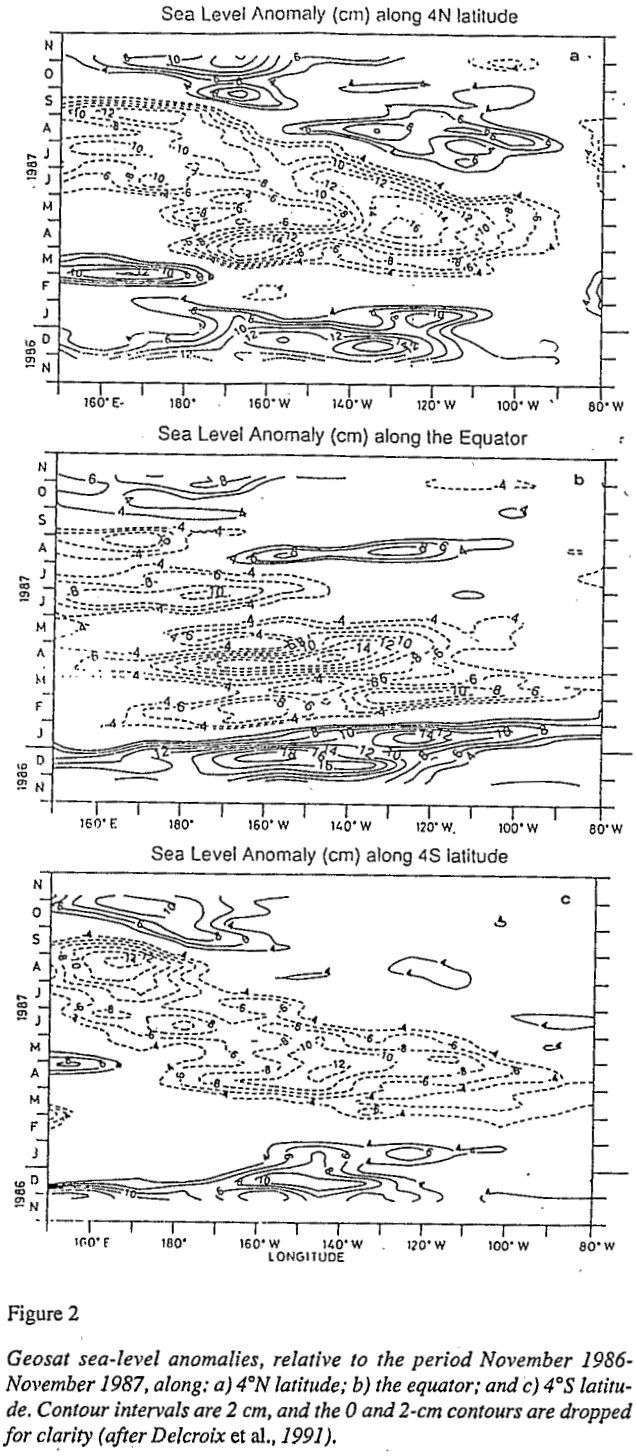

Figure 2

Geosat sea-level anomalies, relative to the period November 1986-November 1987, along: a) 4°N latitude; b) the equator; and c) 4°S latitude. Contour intervals are 2 cm, and the 0 and 2-cm contours are dropped for clarity (after Delcroix et al., *1991).*

Anomalies du niveau de la mer déduites de Geosat, relatives à la période novembre 1986-novembre 1987 : a) le long de 4°N ; b) le long de l'équateur ; c) le long de 4°S. L'intervalle entre deux isolignes est de 2 cm, les isolignes 0 et 2 cm ayant été éliminées pour plus de clarté (d'après Delcroix *et al.*, 1991)

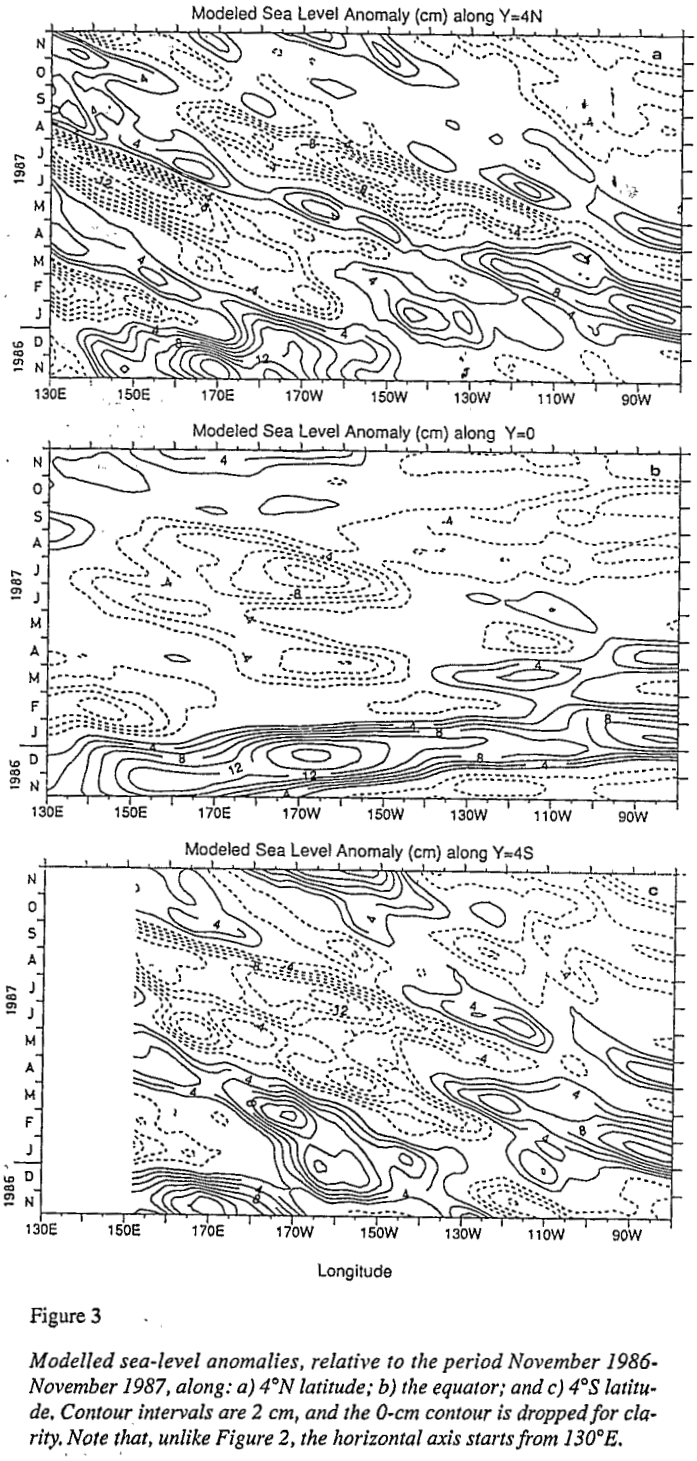

Figure 3

Modelled sea-level anomalies, relative to the period November 1986-November 1987, along: a) 4°N latitude; b) the equator; and c) 4°S latitude. Contour intervals are 2 cm, and the 0-cm contour is dropped for clarity. Note that, unlike Figure 2, the horizontal axis starts from 130°E.

Anomalies du niveau de la mer déduites de Geosat, relatives à la période novembre 1986-novembre 1987 ; a) le long de 4°N ; b) le long de l'équateur ; c) le long de 4°S. L'intervalle entre deux isolignes est de 2 cm, les isolignes 0 et 2 cm ayant été éliminées pour plus de clarté. Noter que l'axe horizontal commence à la longitude 130°E (150°E sur la fig. 2).

here since we focus our study on solving the specific questions raised in the introduction. In other words, the model is used to interpret features which are present both in the modelled and Geosat-derived sea levels. Therefore, as in DPE, three zonal sections are presented to clarify wave propagations: a section at the equator for evidencing Kelvin waves, and sections at 4°N and 4°S where sea level signature of the first-baroclinic, first-meridional mode Rossby wave is maximum.

Wind forcing anomalies, relative to November 1986-November 1987, are presented in Figure 4. Namely, zonal wind stress and Ekman pumping represent the dominant forcing of the local sea level response at and away from the equator, respectively. In parallel, Figures 2 and 3 present the Geosat and model sea-level anomalies along 4°N, the equator and 4°S. At the equator, Geosat data and model results both exhibit a well-marked propagation of the downwelling Kelvin wave, bet-

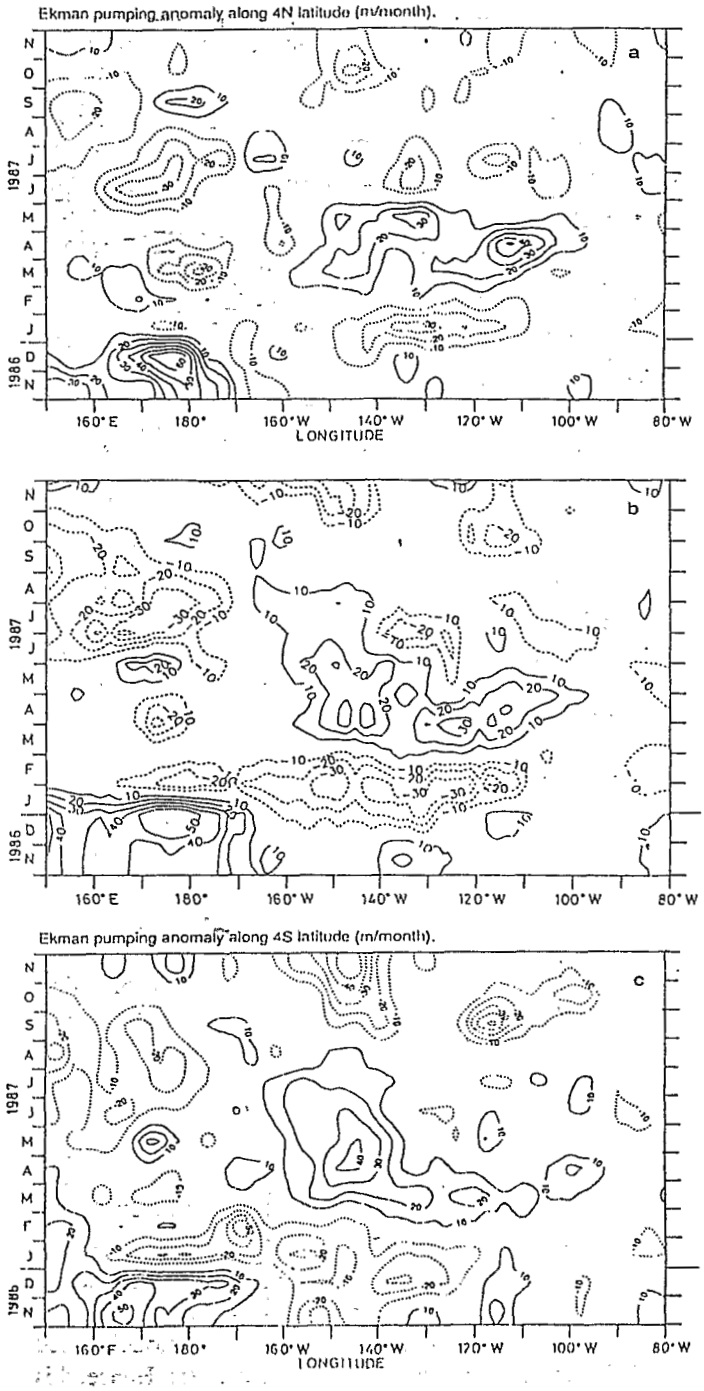

Figure 4

(a) and (c): vertical velocity (m month^{-1}) generated by Ekman pumping anomalies, relative to the period November 1986-November 1987, along the 4°N and 4°S latitudes. Positive values are upward pycnocline motions, i. e., *correspond to negative sea-level variations; (b): zonal wind- stress anomaly, relative to the period November 1986-November 1987, along the equator. Units are 10^3 N/m^2.*

Vitesse verticale de la pycnocline (m mois^{-1}) générée par les anomalies du pompage d'Ekman, relatives à la période novembre 1986-novembre 1987 : a) le long de 4°N; et c) le long de 4°S. Les valeurs positives (vers le haut) correspondent à des variations négatives du niveau de la mer ; b) anomalies de la tension zonale du vent (10^3 N m^{-2}), relatives à la période novembre 1986-novembre 1987, le long de l'équateur.

ween November 1986 and January 1987, with similar sea level signatures and maximum amplitudes (14-16 cm) near 160°-170°W. The Kelvin wave is generated in the western Pacific by westerly wind anomalies (Fig. 4 *b*), and reaches the American coast in January 1987. In Geosat data, an upwelling Kelvin wave, depressing the sea level, follows in January-March 1987 (Fig. 2). This event is not clearly discernible in model results, or, at least, it has a negligible amplitude (0-4 cm) compared to the preceding downwelling Kelvin wave. However, time series of modelled sea level at different equatorial longitudes (Fig. 5) reveal that the upwelling Kelvin wave signal is indeed present in model results between 160°W and the coast of America.

Sections at 4°N and 4°S (Fig. 2 *a* and 2 *c*; 3 *a* and 3 *c*) clearly indicate the occurrence of an upwelling Rossby wave propagating westward from March to September 1987, both in the modelled and Geosat sea level anomalies (12-16 cm maximum anomalies). In the modelled sea level anomalies, a downwelling Rossby wave propagates from the eastern coast in January 1987, up to 130° W (Fig. 3 *a* and 3 *c*). However, west of 130°W, propagation of the downwelling Rossby wave appears only at 4°N with a reduced amplitude. Reflection and propagation of the downwelling wave, consecutive to the downwelling Kelvin wave, does not appear in the Geosat data.

The major long wave activities observed by Geosat during the 1986-1987 El Niño are thus fairly well reproduced by the model. However, differences exist, such as the presence of 30-40 day oscillations, observed in Geosat sea level at 5°N-12°N (Périgaud, 1990). They cannot be simulated in such a linear model.

Figure 5 →

Modelled sea-level anomalies, relative to the period November 1986-November 1987, at the equator and for eight reported longitudes running from 140°E to 80°W. The broken lines give an indication of the propagating downwelling and upwelling Kelvin waves, as discussed in the text. Units are centimetres.

Anomalies du niveau de la mer (en centimètres) calculées par le modèle, relatives à la période novembre 1986-novembre 1987, à l'équateur, pour huit longitudes de 140°E à 80°O. Les lignes en pointillés donnent une indication de la propagation des ondes de Kelvin de downwelling et d'upwelling (*voir* texte).

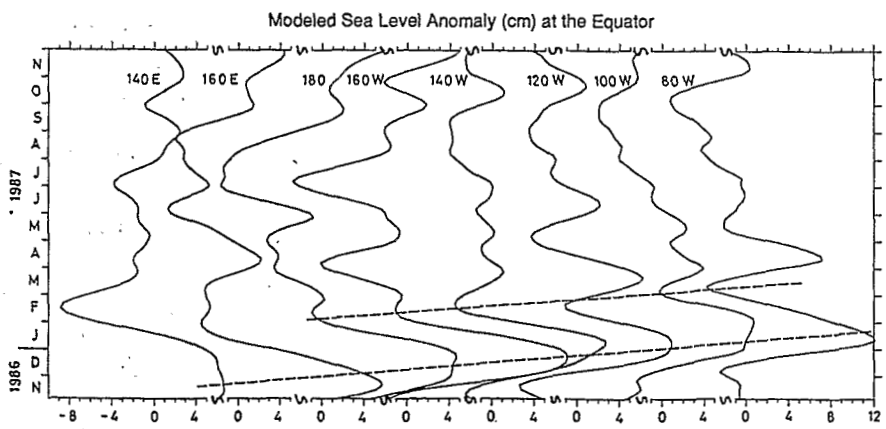

Figure 6

1986-1987 Kelvin wave forcing anomalies along the equator, in non-dimensionnal units (see text).

Anomalies du forçage de l'onde de Kelvin, relatives à la période novembre 1986-novembre 1987, le long de l'équateur, en unités non-dimensionnelles (*voir* texte).

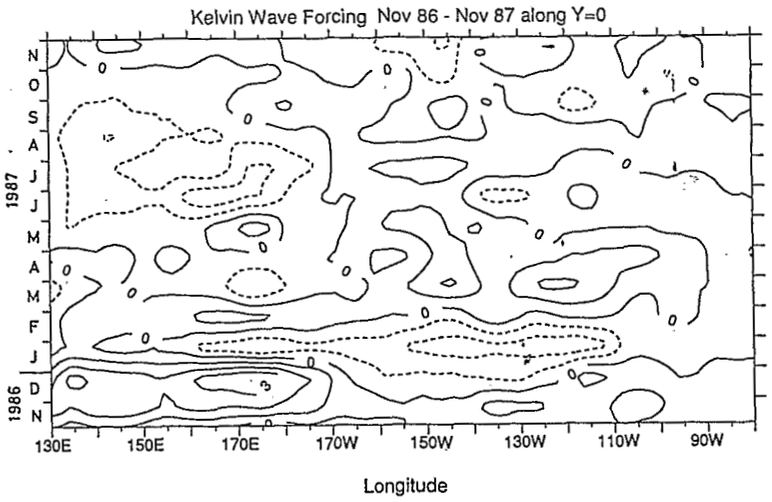

MODEL ANALYSIS

In this section, model results are analysed in order to understand mechanisms which generate the propagating waves, and to answer the questions raised in the introduction.

Eastern boundary reflections

Patches of Ekman pumping anomalies presented at 4°N and 4°S (Fig. 4) are favorable to upwelling between March and May 1987, within 100°-160°W. Such anomalies lower local sea level and may generate upwelling propagation. In other words, the Ekman pumping anomalies may be responsible both for obstructing the downwelling Rossby wave signal and for generating the upwelling Rossby wave observed in Figures 3 *a* and 3 *c*. To test such an assumption, we use the property of the model numerical scheme, namely, the separation between eastward and westward motions (*see* Appendix). The model is run (from 1961 to 1987) in such a way as to obtain only Rossby wave solutions generated by reflections.

For Kelvin wave generation, it is only the zonal wind stress in the vicinity of the equator that matters and the corresponding forcing is simply (*see* Appendix):

$$b_k = 2^{-1/2} \int_{Y_S}^{Y_N} \tau^x (x, y, t)\, \psi_0 (y)\, dy$$

where $\psi_0(y) = (2\pi)^{-1/2} \exp(-y^2)$, $\tau^x (x, y, t)$ is the zonal wind stress and Y_N and Y_S are the northern and southern boundaries of the modelled basin. The forcing in the Kelvin wave equation is unchanged in comparison with the previous experiment. On the other hand, the forcing is set to zero in the system of equations used to solve Rossby wave motions (Appendix, equations A3). Therefore, Rossby wave propagations will only result from Kelvin wave reflections on the eastern boundary.

The Kelvin wave forcing anomalies relative to November 1986-November 1987, presented in Figure 6, depict essentially three events. The first occurs in November-December 1986 when a strong eastward wind stress anomaly takes place between the western coast and about 170°W. It is followed in January 1987 by a strong westward anomaly patch between 110°W and 170°W. Then, in February-March 1987, another patch of westerly wind anomalies is present over most of the basin.

Results of the experiment exhibit a succession of three downwelling and upwelling Kelvin waves propagating along the equator (Fig. 7 *b*). Firstly, a downwelling Kelvin wave, which propagates between November 1986 and January 1987, shows up with a reduced amplitude as compared to model results with full forcing (Fig. 3 *b*). In January 1987, this wave reflects on the eastern coast into Rossby modes, and results in the propagation of a first meridional mode downwelling Rossby wave with sea level maxima at 4°N-4°S (Fig. 7 *a* and 7 *c*). Secondly, in February-March 1987, an upwelling Kelvin wave reflects, and it induces a first meridional mode upwelling Rossby wave with a small sea level signature (0-4 cm range). Thirdly, a downwelling Kelvin wave, generated in March 1987 in the middle of the basin, leads, after reflection, to a well-marked downwelling Rossby wave (6-8 cm range).

In this experiment, a weak upwelling Rossby wave signal appears in the middle of the basin at 4°N and 4°S (Fig. 7 *a* and 7 *c*), in contrast both with results of the model forced with full forcing and with Geosat data analysis. Hence, this experiment indicates that the observed propagating upwelling Rossby wave (March-September 1987; Fig. 2 and 3) mainly owes its existence to Ekman pumping anomalies (Fig. 4 *a* and 4 *c*). The reflection process appears then to be of minor importance although it reinforces the Ekman pumping effect. Moreover, the Ekman pumping helps to cancel the sea level rise due to the downwelling Rossby wave issued from a reflection at the eastern coast in January 1987 (Fig. 3 *b*).

The mean seasonal cycle

Wave activities have been observed with Geosat through their signature in sea level anomalies computed from November 1986 to November 1987. During this period, an El Niño event is underway in the tropical Pacific ocean. In the introduction, the question is posed: do the detected

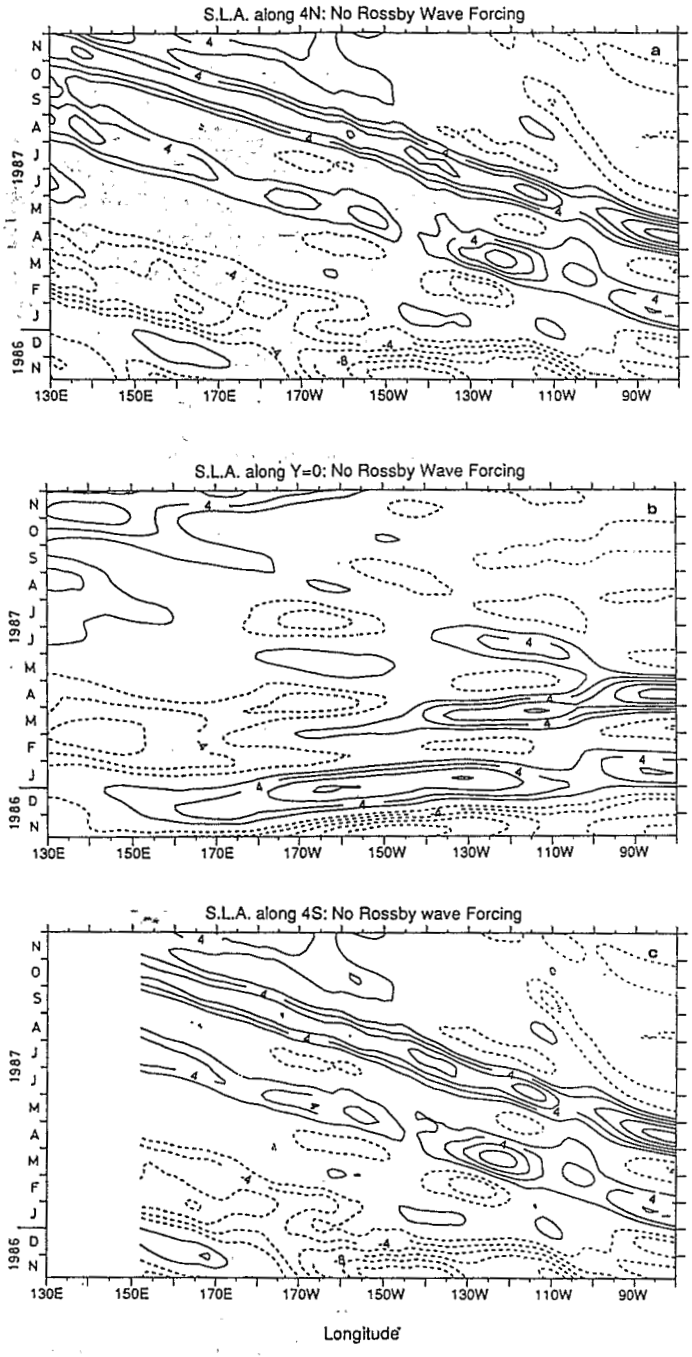

Figure 7

Same as Figure 3, but when the model is forced only with Kelvin wave forcing presented in Figure 6 (see *text*).

Comme figure 3, mais lorsque le modèle est forcé uniquement avec le forçage de Kelvin présenté sur la figure 6 (*voir* texte).

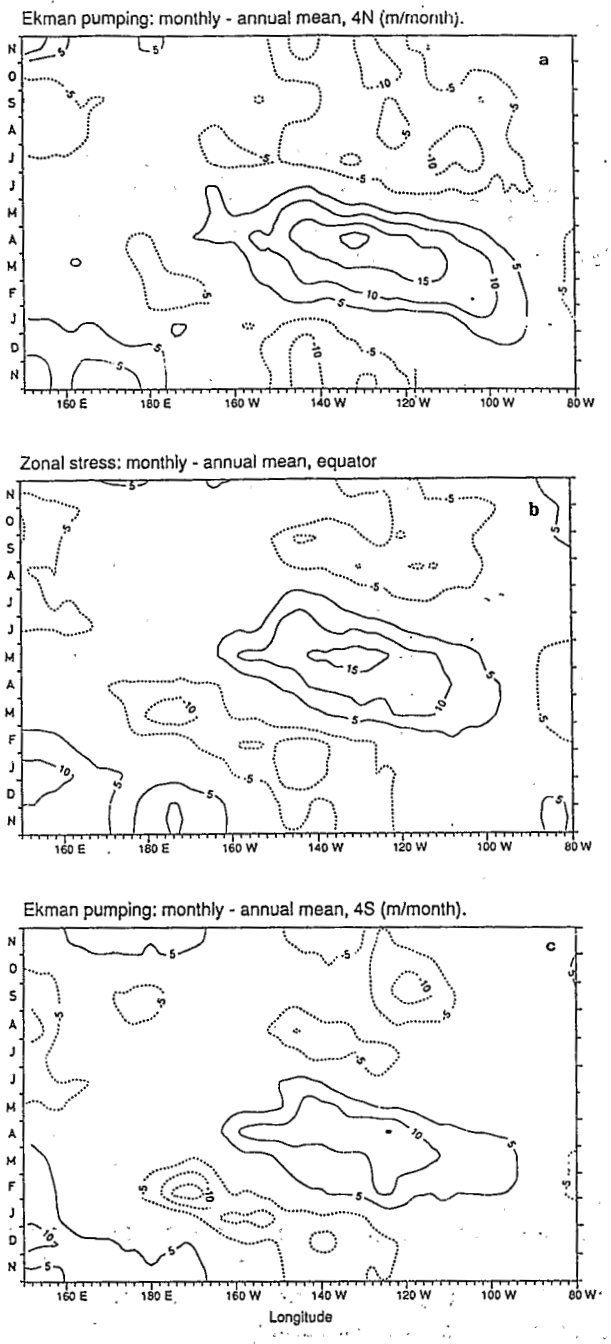

Figure 8

(a) and (c): vertical velocity (m month^{-1}) generated by monthly Ekman pumping anomalies, relative to the climatological annual mean, along the 4°N and 4°S latitudes. Positive values are upward pycnocline motions; (b): monthly zonal wind-stress anomaly, relative to the climatological annual mean, along the equator. Units are 10^3 N/m^2.

(a) et (c) : vitesse verticale de la pycnocline (m mois^{-1}) générée par les anomalies mensuelles du pompage d'Ekman, relatives à la moyenne annuelle climatologique, le long des parallèles 4°N et 4°S. Les valeurs positives (vers le haut) correspondent à des variations négatives du niveau de la mer. (b) : anomalies mensuelles de la tension zonale du vent (10^3 Nm^{-2}) le long de l'équateur, relatives à la moyenne annuelle climatologique.

equatorial Kelvin and Rossby waves belong to the 1986-1987 El Niño or to the mean seasonal cycle ? As mentionned in DPE, this distinction is essential since these equatorial waves strongly affect surface currents, consequently changing the redistribution of mass and heat over the entire tropical basin.

Seasonal wind stress anomalies (relative to the annual mean) have been computed from the 1961-1988 FSU file. The corresponding zonal wind stress (Fig. 8 *b*) exhibits, in the western equatorial Pacific, a period of westerly anomalies in November-January. Such anomalies are thus potentially able to generate downwelling Kelvin waves which propagate along the equator. Around 4°N and 4°S, Ekman pumping anomalies are favourable to upwelling between roughly 100°-160°W and February-April (Fig. 8 *a* and 8 *c*). Such a forcing is susceptible to generate upwelling

Rossby waves. To assess wether these wind features may generate wave activities comparable to those observed in 1986-1987, the model is then forced with the mean seasonal wind stress.

Along the equator (Fig. 9 *b*), as expected from the wind forcing, an annual downwelling Kelvin wave propagates between November and January, and results in a 2-6 cm sea level rise. There is some evidence of an upwelling Kelvin wave in March-April, starting from the central Pacific. The 1986-1987 succession of downwelling and upwelling Kelvin waves thus appears to be part of the mean seasonal cycle. However, the amplitude of the annual downwelling Kelvin wave is enhanced in austral summer 1986-1987 (Fig 3 *b*). At that time, westerly wind anomalies extend further east and are stronger than the corresponding mean seasonal anomalies (Fig. 5 *b* and 8 *b*).

The reflection of the annual downwelling Kelvin wave at the eastern coast, as a westward propagating Rossby wave, is slightly visible during December- January at 4°N and 4°S (Fig. 9 *a* and *c*). This downwelling Rossby wave does not propagate very far off the coast. It is followed, in March-October, by a westward propagating upwelling Rossby wave (10 cm maximum) between 120°W-150°E. This wave corresponds to the annual upwelling Rossby wave detected, with BT and XBT measurements, only in the northern hemisphere as a result of poor data coverage in the southern hemisphere (Meyers, 1979; Kessler, 1990). As mentioned above, the upwelling-favourable Ekman pumping generates the annual propagating Rossby wave, and also inhibits the propagation of the downwelling reflected Rossby wave. The 1986-1987 Rossby wave propagations, described in the previous section, are thus part of the mean seasonal cycle. However, the amplitude of the downwelling Rossby wave, issued from the reflection, is enhanced in 1986-1987, and the wave propagates farther west than during the mean year (Fig. 3 *a* and 3 *b*, as compared to Fig. 9 *a* and 9 *b*). The 1986-1987 upwelling Rossby wave is characterized by a maximum sea level amplitude slightly greater than during the mean seasonal cycle (2 to 4 cm differences). In March-May 1987, the Ekman pumping anomalies at 4°N and 4°S are twice as strong as normal (Fig. 5 and 7), and one would expect an upwelling Rossby wave response in the same ratio. However, the Ekman pumping in 1987 also acts to cancel the downwelling Rossby sea level rise issued from the reflection of the stronger-than-normal November-December 1986 Kelvin wave.

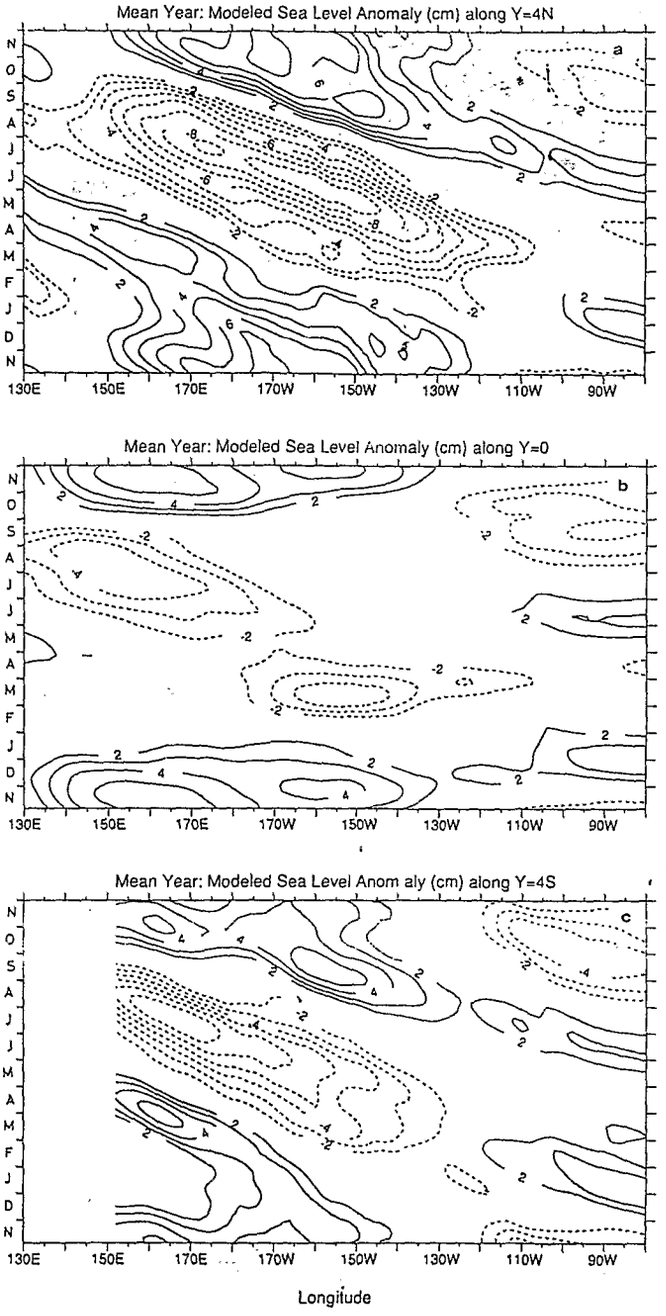

Figure 9

Monthly modelled sea-level anomalies, relative to the climatological annual mean, along: a) 4°N latitude; b) the equator; and c) 4°S latitude. Contour intervals are 2 cm, and the 0-cm contour is dropped for clarity.

Anomalies mensuelles du niveau de la mer (en centimètres) calculées par le modèle, relatives à la moyenne annuelle climatologique : a) le long de 4°N ; b) le long de l'équateur ; et c) le long de 4°S. L'intervalle entre deux isolignes est de 2 cm, les isolignes 0 et 2 cm ayant été éliminées pour plus de clarté.

CONCLUSION

In the present study, interpretation of propagating equatorial waves, as detected with Geosat sea level data, is based on results of a numerical model forced by the FSU wind stress. Both model and wind stress have their own limitations. The model is a simple linear model which does not take into account thermodynamic effects, and it simplifies the ocean to a two-layer system. Wind measurements from ship reports are obviously limited in time and space, and the derived wind stress field is subject to errors inherent in the analysis procedures (*see* Busalacchi *et al.*, 1990, for sensitivity experiments with a similar model forced by different wind fields). In addition, it should be borne in mind that Geosat measurements are also subject to environmental and instrumental errors (*e. g.*, Cheney *et al.*, 1989).

Despite all these limitations, the major wave activities evidenced by Geosat, during the 1986-1987 El Niño, present interesting similarities with our model results. Namely,

from December 1986 to January 1987, a well-marked downwelling Kelvin wave propagates across the equatorial basin. It is followed in February-March 1987 by an upwelling Kelvin wave with a more pronounced sea level amplitude in Geosat data than in model results. Also, during March-September 1987, a first meridional mode upwelling Rossby wave propagates all across the basin.

The relative importance of local forcing and reflection processes in generating the upwelling Rossby wave is investigated using specific modelling experiments. It appears that upwelling-favourable wind forcing in the eastern part of the equatorial basin is the main mechanism generating the upwelling Rossby wave. The reflection of the upwelling Kelvin wave is of secondary importance in this generation. However, it contributes to the upwelling Rossby wave signal, and makes it visible all the way from the eastern to the western sides of the equatorial Pacific.

All the 1986-1987 propagating features are present in the mean seasonal cycle, with the exception that an upwelling Kelvin does not immediately follow the downwelling Kelvin wave in January. We conclude that the 1986-1987 El Niño wave activity is phase-locked to the mean seasonal cycle. However, the downwelling Kelvin wave and, to a lesser extent, the upwelling Rossby wave have a greater amplitude during the 1986-1987 El Niño than during the mean year. This stems from the fact that, in November 1986, the westerly wind stress anomaly observed in the western equatorial Pacific is stronger and extends further west than normal, and that, in March-April 1987, the Ekman pumping around 110°-150°W is twice the normal extent.

The enhancement of the downwelling Kelvin and upwelling Rossby waves has noticeable effects on the tropical Pacific circulation during the 1986-1987 El Niño, since both waves are characterized by eastward surface flow anomalies (DPE). In particular, as suggested in McPhaden and Picaut (1990) and demonstrated in Delcroix *et al.* (1992), both waves do contribute to the eastward displacement and draining of the western Pacific warm pool, thought to be of principal importance in El Niño-Southern Oscillation phenomena.

Despite the short period of the analysed Geosat data (thirteen months), satellite altimeter measurements, combined with a numerical model, proved to be very valuable in the present study, which addresses and solves questions directly related to the intrinsic mechanisms responsible for low-frequency ocean variations. The future Topex/Poseidon mission, with unprecedented high-quality sea level coverage over several years, will undoubtedly refine and extend our analysis.

Acknowledgements

The Florida State University wind stress data were kindly provided by Professor J.J. O'Brien. Contributions from G. Eldin were appreciated. Support for this work, as part of the Topex/Poseidon Science Working Team, was provided by the Programme National de Télédétection Spatiale, through Actions Incitatives sur Programmes 9.88.25 and 91N50/0550.

Appendix

The model is described in detail in Cane and Patton (1984). It solves the scaled shallow-water equations using the long-wave low frequency approximation:

$$\frac{\partial u}{\partial t} - yv + \frac{\partial h}{\partial x} = \tau^x$$

$$yu + \frac{\partial h}{\partial y} = \tau^y \qquad \text{(A1)}$$

$$\frac{\partial h}{\partial t} + \frac{\partial u}{\partial x} + \frac{\partial v}{\partial y} = 0$$

where all notations are standard, with τ^x and τ^y being the zonal and meridional components of the wind stress.

High-frequency inertia-gravity waves and short wavelength Rossby waves are filtered out. The wave solutions to these equations form a complete and orthogonal set (Cane and Sarachick, 1977; 1981). An inner product is defined as:

$$[(u^a, v^a, h^a) \cdot (u^b, v^b, h^b)] \equiv \int_{-\infty}^{+\infty} (u^a u^b + v^a v^b + h^a h^b)\, dy$$

The Kelvin mode is orthogonal to all other modes. Therefore, the total solution can be written as:

$$(u, v, h) = a_k (x, t)\, (\psi_0 (y), 0, \psi_0 (y)) + [u' (x, y, t), v' (x, y, t), h' (x, y, t)]$$

where $a_k (x, t)$ is the amplitude of Kelvin waves and the prime quantities denote the long Rossby and anti-Kelvin modes propagating westward. Projecting equations (A1) on to the Kelvin solution leads to:

$$\frac{\partial a_k}{\partial t} + \frac{\partial a_k}{\partial x} = b_k (x, t) \qquad \text{(A2)}$$

$$\text{with } b_k = \frac{[(\tau^x, \tau^y, 0) \cdot (\psi_0, 0, \psi_0)]}{[(\psi_0, 0, \psi_0) \cdot (\psi_0, 0, \psi_0)]}$$

$$= 2^{-1/2} \int_{Y_S}^{Y_N} \tau^x (x, y, t)\, \psi_0 (y)\, dy$$

The rest of the solution is governed by the set of equations obtained in substracting the Kelvin wave equation from equations (A1):

$$\frac{\partial u'}{\partial t} - yv' + \frac{\partial h'}{\partial x} = \tau^x - b_k \psi_0$$

$$yu' + \frac{\partial h'}{\partial y} = \tau^y \qquad \text{(A3)}$$

$$\frac{\partial h'}{\partial t} + \frac{\partial u'}{\partial x} + \frac{\partial v'}{\partial y} = -b_k \psi_0$$

REFERENCES

Busalacchi A.J. and J.J. O'Brien (1981). Interannual variability of the equatorial Pacific in the 1960's. *J. geophys. Res.*, **86**, 10901-10907.

Busalacchi A.J. and M.A. Cane (1985). Hindcasts of sea level variations during the 1982-1983 El Niño. *J. phys. Oceanogr.*, **15**, 213-221.

Busalacchi A.J., M.J. McPhaden, J. Picaut and S.R. Springer (1990). Sensitivity of wind-driven tropical Pacific Ocean simulations on seasonal and interannual time scales. *J. mar. Syst.*, **1**, 119-154.

Cane M.A. (1984). Modelling sea level during El Niño. *J. phys. Oceanogr.*, **14**, 1864-1874.

Cane M.A. and E.S. Sarachick (1977). Forced baroclinic ocean motions. II: The linear bounded case. *J. mar. Res.*, **42**, 487-502.

Cane M.A. and E.S. Sarachick (1981). The response of a linear baroclinic ocean to periodic forcing. *J. mar. Res.*, **39**, 651-693.

Cane M.A. and R.J. Patton (1984). A numerical model for the low frequency equatorial dynamics. *J. phys. Oceanogr.*, **14**, 1853-1863.

Cheney R.E., B.C. Douglas and L. Miller (1989). Evaluation of Geosat altimeter data with application to tropical Pacific sea-level variability. *J. geophys. Res.*, **94**, 4737-4749.

Delcroix T., J. Picaut and G. Eldin (1991). Equatorial Kelvin and Rossby waves evidenced in the Pacific Ocean through Geosat sea level and surface current anomalies. *J. geophys. Res., Suppl.*, **96**, 3249-3262.

Delcroix T., G. Eldin, M.H. Radenac, J. Toole and E. Firing (1992). Variations of the western equatorial Pacific Ocean, 1986-1988. *J. geophys. Res.*, **97**, 5423-5445.

Douglas B.C. and R.E Cheney (1990). Geosat: beginning a new era in satellite oceanography. *J. geophys. Res.*, **95**, 2833-2836.

Goldenberg S.B. and J.J. O'Brien (1981). Time and space variability of tropical wind stress. *Mon. Weath. Rev.*, **109**, 1190-1207.

Kessler W.S (1990). Observations of long Rossby waves in the northern tropical Pacific. *J. geophys. Res.*, **95**, 5183-5217.

Knox R. and D. Halpern (1982). Long-range Kelvin wave propagation of transport variations in Pacific Ocean equatorial currents. *J. mar. Res., Suppl.*, **40**, 329-339.

Lukas R, S.P. Hayes and K. Wyrtki (1984). Equatorial sea-level response during the 1982-1983 El Niño. *J. geophys. Res.*, **89**, 10425-10430.

McPhaden M.J. and S.P. Hayes (1990). Variability in the eastern equatorial Pacific Ocean during 1986-1988. *J. geophys. Res.*, **95**, 13195-13208.

McPhaden M.J. and J. Picaut (1990). El Niño-southern oscillation displacements of the western equatorial Pacific warm pool. *Science*, **250**, 1385-1388.

Meyers G. (1979). On the annual Rossby wave in the tropical north Pacific Ocean. *J. phys. Oceanogr.*, **9**, 663-674.

Miller L., R.E. Cheney and B.C. Douglas (1988). Geosat altimeter observations of Kelvin waves and the 1986-1987 El Niño. *Science*, **239**, 52-54.

du Penhoat Y. and A.-M. Tréguier (1985). The seasonal response of the tropical Atlantic Ocean. *J. phys. Oceanogr.*, **15**, 316-329.

Périgaud C. (1990). Sea-level oscillations observed with Geosat along the two shear fronts of the Pacific North Equatorial Countercurrent. *J. geophys. Res.*, **95**, 7239-7248.

Picaut J., A.J. Busalacchi, M.J. McPhaden and B. Camusat (1990). Validation of the geostrophic method for estimating zonal currents at the equator from Geosat altimeter data. *J. geophys. Res.*, **95**, 3015-3024.

Rébert J.P., J.R. Donguy, G. Eldin and K. Wyrtki (1985). Relations between sea level, thermocline depth, heat content and dynamic height in the tropical Pacific Ocean. *J. geophys. Res.*, **90**, 11719-11725.

Coden OCACD 9
ISSN 0399 1784

OCEANOLOGICA ACTA

European Journal of Oceanology
Revue Européenne d'Océanologie

Volume 15/N° 5
1992

gauthier-villars

SATELLITE ALTIMETRY FOR OCEANOGRAPHY
From Data Processing To Data Assimilation

Edited by J. Verron